Robust ILC Design with Application to Stroke Rehabilitation

C. T. Freeman,

Electronics and Computer Science, University of Southampton, United Kingdom

Abstract

Iterative learning control (ILC) is a design technique which can achieve accurate tracking by learning over repeated task attempts. However, long-term stability remains a critical limitation to widespread application, and to-date robustness analysis has overwhelmingly considered structured uncertainties. This paper substantially expands the scope of existing ILC robustness analysis by addressing unstructured uncertainties, a widely used ILC update class, the presence of a feedback controller, and a general task description that incorporates the most recent expansions in the ILC tracking objective. Gap metric based analysis is applied to ILC by reformulating the finite horizon trial-to-trial feedforward dynamics into an equivalent along-the-trial feedback system, as well as deriving relationships to link their respective gap metric values. The results are used to generate a comprehensive design framework for robust control design of the interacting feedback and ILC loops. This is illustrated via application to rehabilitation engineering, an area where they meet an urgent need for high performance in the presence of significant modeling uncertainty.

Key words: Iterative learning control; robustness; electrical stimulation; rehabilitation engineering.

1 Introduction

The iterative learning control (ILC) paradigm addresses tracking of a fixed reference trajectory over a finite time interval of T seconds. Each attempt is termed a 'trial', and the system is reset between trials to the same starting position. The tracking error is recorded during each trial, and in the reset period is used to update the control signal with the aim of reducing the error during the subsequent trial. ILC was originally developed to enable precision control of industrial robotics, but now covers a rich theoretical framework and broad range of applications, see e.g. [5,1]. While impressive tracking performance is achievable on nominal systems and satisfactory performance has been achieved in practical applications, robustness remains a serious issue. In practice it has been found that long term instabilities degrade the performance and convergence of the standard algorithms.

ILC long term stability is not well understood, and a variety of methods (e.g. quantisation, filtering, suspension of learning) have been proposed to address the commonly encountered problem of convergence, followed by rapid divergence. These often lack theoretical basis and there remains debate on the cause of this phenomenon. Previous robustness results relate to multiplicative and additive uncertainty descriptions [20,16,26,24,6,10], or to parametric uncertainty [2]. Unstructured uncertainties were addressed in [8] where it was shown that there exists a non-zero stability margin for a class of adaptive ILC algorithms. However, the analysis was not extended to more general ILC update classes. It is hence desirable for a general framework to quantify the effect of realistic model mismatch, thereby informing practical design. Furthermore, there is also a need to incorporate recent expansion in the ILC framework in which the tracking objective is generalized to permit tracking only at isolated time-points or over intervals in $[0,T]$ [23,11,19]. This expanded class meet the needs of a wide range of industrial processes, such as robotic pick-and-place tasks, welding, and coordinated motion. However, the only robustness results for this expanded task framework relate to multiplicative uncertainty [18].

This paper substantially expands the scope of existing ILC robustness analysis by addressing for the first time: (1) unstructured uncertainties, (2) a general ILC update class, and (3) a full generalization of the task descriptions that have so far been considered in ILC. To maximize impact, we also consider inclusion of a feedback controller. Analysis is based on the nonlinear gap metric of [9], which is applied to ILC by reformulating the within-in trial feedforward action as trial to trial feedback action. The resulting gap on the trial to trial dynamics is then translated back to the original plant.

This paper is arranged as follows: a general problem description is defined in Section 2, and robust performance analysis is undertaken in Section 3 with proofs contained in the appendix. To illustrate the power of the framework, results are presented in Section 4 from an application to stroke rehabilitation. Section 5 contains conclusions and topics of future work.

Email address: cf@ecs.soton.ac.uk (C. T. Freeman).

2 Problem Description

We consider the general along-the-trial system mapping

$$N : \mathscr{L}_2^m[0,T] \to \mathscr{L}_2^p[0,T] : u_k \mapsto y_k,\ N(0) = 0 \quad (1)$$

which is assumed bounded-input, bounded-output (BIBO) stable. Subscript $k \in \mathbb{N}_+$ denotes the trial number, and the control structure is shown in Figure 1. Feedback controller

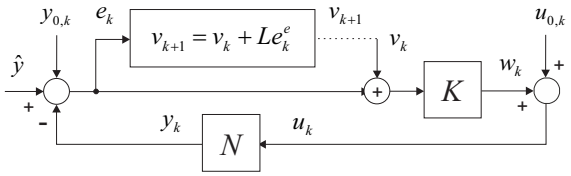

Fig. 1. ILC and feedback control structure with true system N.

mapping

$$K : \mathscr{L}_2^p[0,T] \to \mathscr{L}_2^m[0,T] : (e_k + v_k) \mapsto w_k,\ K(0) = 0 \quad (2)$$

is used to provide baseline performance and rejection of external disturbances $u_{0,k}$, $y_{0,k}$. The closed loop $[N,K]$ is assumed well-posed, and the standard control problem is for plant output y_k to track a reference signal $\hat{y} \in \mathscr{L}_2^p[0,T]$ as k increases. In ILC, this is achieved by successively updating feedforward signal v_k using the tracking error $e_k = \hat{y} + y_{0,k} - y_k$. Tracking over the full duration $[0,T]$ is often unnecessary, and hence we consider the more general case of tracking q sub-intervals (i.e. $[t_{j-1},t_j]$, $j = 1 \cdots q$ where $0 = t_0 \le t_1 \le \cdots T_q = T$ are distinct points in $[0,T]$), or at isolated time points (i.e. setting $t_{j-1} = t_j$). This generalization covers the most recent expansions in the ILC task, e.g. [23,11,19]. To include all these cases, we introduce a projection operator

$$P : \mathscr{L}_2^p[0,T] \to \mathscr{L}_2^{p_1}[0,t_1] \times \cdots \times \mathscr{L}_2^{p_q}[t_{q-1},t_q] : y \mapsto \begin{bmatrix} (Py)_1 \\ \vdots \\ (Py)_q \end{bmatrix}$$
$$((Py)_j)(t) = P_j y(t),\ t \in [t_{j-1},t_j],\ j = 1,\cdots,q \quad (3)$$

to extract the required sub-interval components, where P_j is a $p_j \times p$ matrix of full row rank specifying the output components involved in movement stipulated over time interval $[t_{j-1},t_j]$. The control objective is therefore

$$\lim_{k\to\infty} v_k = v_\infty, \qquad v_\infty := \min_{v_k} \|\hat{y}^e - y_k^e\|^2 \quad (4)$$

where the 'extended' reference and output are $\hat{y}^e = P\hat{y}$ and $y_k^e = Py_k$ respectively. The standard ILC objective of minimizing $\|e_k\|^2$ is restored by setting $P = I$ (via $q = 1$, $t_1 = T$, $P_1 = I$). To achieve (4), we consider the ILC update structure

$$v_{k+1} = v_k + Le_k^e, \qquad k = 0,1,\cdots \qquad v_0 = 0 \quad (5)$$

where operator $L : \mathscr{L}_2^{p_1}[0,t_1] \times \cdots \times \mathscr{L}_2^{p_q}[t_{q-1},t_q] \to \mathscr{L}_2^p[0,T]$, $L(0) = 0$. Suppose L is designed based on a linear, potentially unstable, approximation, $M : \mathscr{L}_2^m[0,T] \to \mathscr{L}_2^p[0,T]$, to the true plant dynamics N. The following result is an extension of existing ILC convergence criteria to include the extended task description of (3) and the general case of MIMO dynamics with arbitrary input and output dimensions.

Proposition 2.1 *Let linear operator K be designed such that the closed-loop $[M,K]$ is gain stable, and let ILC update sequence (5) be applied with L satisfying induced norm bound*

$$\|I - PGL\| = \gamma < 1 \quad (6)$$

where $G = (I+MK)^{-1}MK$, then objective (4) holds with

$$v_\infty := \lim_{k\to\infty} v_k = L(PGL)^{-1}\hat{y}^e - \hat{y},\ y_\infty^e := \lim_{k\to\infty} y_k^e = \hat{y}^e. \quad (7)$$

Alternatively, if ILC operator L is chosen to satisfy

$$\|I - LPG\| = \gamma < 1 \quad (8)$$

then the ILC update signal converges as

$$v_\infty := \lim_{k\to\infty} v_k = (LPG)^{-1}L\hat{y}^e - \hat{y}. \quad (9)$$

Note that necessary and sufficient conditions for the existence of an operator L to satisfy (6) and (8) for an arbitrary reference $\hat{y}^e$ are respectively

$$\mathrm{Im}(PG) = \mathscr{L}_2^{p_1}[0,t_1] \times \cdots \times \mathscr{L}_2^{p_q}[t_{q-1},t_q] \Leftrightarrow \ker((PG)^*) = \{0\}, \quad (10)$$
$$\ker(PG) = \{0\} \Leftrightarrow \mathrm{Im}((PG)^*) = \mathscr{L}_2^p[0,T] \quad (11)$$

where $(PG)^* = G^*P^*$ is the adjoint of operator PG. Having designed K and L based on the approximate model M, we now establish their robust performance when applied to the true plant N. To do this it is necessary to embed the ILC trial-to-trial update dynamics and the feedback controller along-the-trial dynamics within a single system description.

3 Robust Performance

The nonlinear gap metric, δ, is an established measure of distance between two systems [9]. To apply gap based robust stability results to ILC, it is first necessary to reformulate the finite-duration along-the-trial feedforward dynamics as a trial to trial feedback system with discrete-time sample instant k. Then the resulting conditions must be translated back to the original along-the-trial system. First express the dynamics over $t \in [0,T]$ of the k^{th} trial as a single time instant of a so-called 'lifted' system, by writing the signals appearing in Figure 1 as

$$v_k = v(k),\ e_k = e(k),\ y_k = y(k),\ y_{0,k} = y_0(k) \in \mathscr{L}_2^p[0,T],$$
$$u_k = u(k),\ u_{0,k} = u_0(k) \in \mathscr{L}_2^m[0,T], \quad (12)$$

and then define the corresponding lifted signal spaces

$$v,\ e,\ y \in \mathscr{L}_2^p[0,T] \times \mathbb{N}, \quad u \in \mathscr{L}_2^m[0,T] \times \mathbb{N}.$$

Trial-to-trial operators $\bar{N}$, $\bar{K}$, $\bar{L}$ can then be expressed in terms of their along-the-trial counterparts as:

$$\bar{N} : \mathscr{L}_2^m[0,T] \times \mathbb{N} \to \mathscr{L}_2^p[0,T] \times \mathbb{N} : u \mapsto y : y(k) = Nu(k) \quad (13)$$

$$\bar{K} : \mathscr{L}_2^p[0,T] \times \mathbb{N} \to \mathscr{L}_2^m[0,T] \times \mathbb{N} : (v+e) \mapsto w : w(k) = K(v(k)+e(k)), \quad (14)$$

$$\bar{L} : \mathscr{L}_2^p[0,T] \times \mathbb{N} \to \mathscr{L}_2^p[0,T] \times \mathbb{N} : e \mapsto v : v(k+1) = v(k) + LPe(k), v(0) = 0 \quad (15)$$

for $k \in \mathbb{N}_+$. Similarly, $\bar{M}$ is obtained by replacing N by M in (13). Now define

$$\bar{C} : \mathscr{L}_2^p[0,T] \times \mathbb{N} \to \mathscr{L}_2^m[0,T] \times \mathbb{N} : e \mapsto w : w = \bar{K}(\bar{L}+I)e. \tag{16}$$

The trial-to-trial system is shown in Figure 2, with dynamics

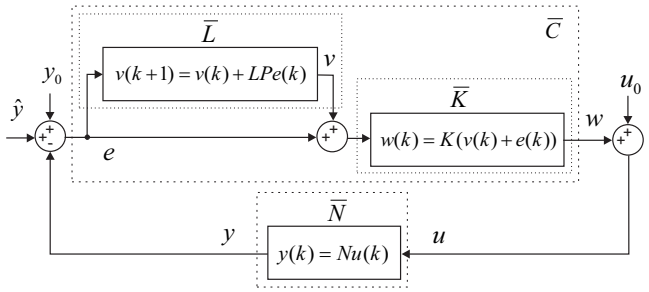

Fig. 2. ILC and feedback control scheme $[\bar{N},\bar{C}]$.

$$\Pi_{\bar{N}//\bar{C}} : \begin{pmatrix} u_0 \\ y_0 + \hat{y} \end{pmatrix} \mapsto \begin{pmatrix} u \\ y \end{pmatrix} \quad \text{with} \quad \begin{pmatrix} \bar{u}_k \\ \bar{y}_k \end{pmatrix} = \Pi_{\bar{N}//\bar{C}} \begin{pmatrix} 0 \\ \hat{y} \end{pmatrix}(k).$$

Since (12)-(16) defines a dynamic system in lifted space, it is possible to derive the robust performance results for the case where the control scheme operates with the true plant.

Theorem 3.1 *Let L be designed to satisfy either (6) or (8) of Theorem 2.1. Then the true combined feedback and ILC system $[\bar{N},\bar{C}]$ is BIBO stable if the biased gap satisfies*

$$\delta(\bar{M},\bar{N}) < b_{\bar{M}//\bar{C}}^{-1} \tag{17}$$

where the gain bound associated with $[\bar{M},\bar{C}]$ is

$$b_{\bar{M}//\bar{C}} = \frac{\left\| \begin{pmatrix} I \\ M \end{pmatrix} K(I+MK)^{-1} \right\| \|L\| \left\| P(I+MK)^{-1}(-M,I) \right\|}{1-\gamma} + b_{M//K} \tag{18}$$

with the purely feedback component (i.e. $L = 0$) given by

$$b_{M//K} = b_{\bar{M}//\bar{K}} = \left\| \begin{pmatrix} I \\ M \end{pmatrix} (I+KM)^{-1}(I,K) \right\|. \tag{19}$$

In particular, convergence of the true system satisfies

$$\|\Pi_{\bar{N}//\bar{C}}\|_{\begin{pmatrix} 0 \\ \hat{y} \end{pmatrix}} \leq b_{\bar{M}//\bar{C}} \frac{1+\delta(\bar{M},\bar{N})}{1-b_{\bar{M}//\bar{C}}\delta(\bar{M},\bar{N})}. \tag{20}$$

Proof: See Appendix A. □

The interpretation of condition (17) is that the proposed controller stabilizes a 'ball' of plants in the uncertainty space centred about the nominal system model $\bar{M}$. The radius of this ball is $b_{M//K}^{-1}$ in the case of feedback action alone, but reduces when ILC action is added (due to the introduction of the additional term on the right hand side of (18)). Note that the right hand side of (18) is always finite if $\|L\|$ is bounded, so the radius of this ball is always greater than zero and increases in size as $\|L\|$ reduces to zero. This means that Theorem 3.1 provides a transparent method to design both the feedback and ILC controller components to weigh performance against robustness. The next result translates the gap metric between lifted systems $\bar{M}$, $\bar{N}$ to the standard along-the-trial gap metric between original systems M, N.

Theorem 3.2 *The gap measure of mismatch between lifted system operators $\bar{M}$ and $\bar{N}$ can be related to the mismatch between their respective unlifted counterparts M and N via*

$$\delta(\bar{M},\bar{N}) \leq \delta(M,N) \leq \sup_{\|u\| \neq 0,\, k \in \mathbb{N}_+} \frac{\|(N|_{\bar{u}_k} - M)u\|}{\|u\|}. \tag{21}$$

where $\delta(M,N)$ is the biased gap between unlifted systems.

Proof: See Appendix B. □

Hence we can replace $\delta(\bar{M},\bar{N})$ by either $\delta(M,N)$ or $\sup_{k\in\mathbb{N}_+} \|N|_{\bar{u}_k} - M\|$ throughout Theorem 3.1. Theorem 3.1 provides explicit conditions guaranteeing robust performance, and relationships (21) enable straightforward computation using the standard along-the-trial operators M and N. Together, these motivate Design Procedure 1, which is a major extension of existing ILC robustness results: not only are robust performance bounds given for unstructured uncertainties, but the results also clearly show the effect of the tracking objective, feedback controller, and ILC update design. Condition (20) bounds convergence with respect to (u_k, y_k) which are related to the ideal nominal signals (e.g. those appearing in (7), (9)) via continuous function Ψ defined in (B.1). Figure 3 summarises the control design procedure for stabilisation of an unknown true plant.

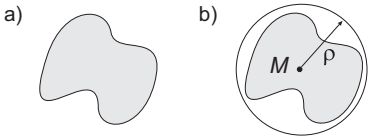

Fig. 3. Design procedure: a) uncertainty space known to contain true plant N, b) stabilised ball of plants with radius $\rho = b_{\bar{M}//\bar{C}}^{-1}$.

4 Design Procedure Application Example

The power and generality of the results are now illustrated by applying them to the field of stroke rehabilitation. This is an area of intense current interest but one in which accurate model identification is challenging. We first show how ILC operator L can be computed to satisfy (6) in the case that (10) holds, or to satisfy (8) in the case that (11) holds.

Theorem 4.1 *Within (5) let the ILC operator be given by*

$$L = (PG)^* \left(I + PG(PG)^*\right)^{-1}. \tag{22}$$

Design Procedure 1 : Guidelines for robust stability

Define task : If feasible in practice, reduce the time intervals or isolated instants over which tracking is required such that the resulting task objective operator, P has minimal norm.

Select feedback controller : Select feedback action K to provide baseline tracking and disturbance rejection while minimizing $b_{M,K}$ given by (19).

Select ILC algorithm : Compute an ILC operator L to satisfy (6), (8) within Theorem 2.1. To maximize robustness, this must minimize the right hand side of (18), which requires that both L and γ are minimised. Reducing both L and γ corresponds to slower convergence, and can be made arbitrarily small if convergence speed is not an issue.

Inspect robust uncertainty : Compute $b^{-1}_{\tilde{M}//\tilde{C}}$ using (18) and compare against realistic cases of model uncertainty found using the right-hand term in (21). If the radius of the 'ball' of stabilized plants is too small, then compute alternative feedback and ILC controllers.

Experimental evaluation : Implement the controller, measure and quantify performance. If necessary, redefine the task (to reduce $\|P\|$), slow learning (to reduce $\|L\|$) or de-tune feedback tracking performance (to reduce $b_{M//K}$) in order to increase the radius of the stabilized ball of plants. Alternatively, re-identify the plant model M to reduce the mismatch, $\delta(M,N)$, between it and the true system N.

If (10) holds, then (6) is satisfied and furthermore v_∞ is the minimum input solution to (4), i.e.

$$v_\infty := \min_{v_k} \|v_k\|^2 \ \ s.\ t.\ \ e^e_k = 0 \tag{23}$$

Alternatively, if (11) holds, then (8) is satisfied, and v_∞ additionally solves (4).

Proof: This can be shown by extending the Hilbert space optimality analysis of [18], and by embedding within it the projection operator P defined by (3). □

4.1 Rehabilitation System Description

Upper limb rehabilitation requires neurologically impaired participants to repeatedly perform tracking movements with their affected arm, with a rest period in between attempts. In recent years there has been a shift towards model-based control design of electrical stimulation (ES) and robotic therapy (RT) which are used to facilitate the intense, goal-orientated training of movement tasks that is needed for effective recovery. The repetitive nature of the rehabilitation process has led to a significant number of clinical studies involving ILC [21,17,4,3,22,12] to control the assistance. However, the difficulty of accurately identifying a model in clinical practice makes robust ILC Design Procedure 1 highly valuable.

Let u denote the m ES signals applied to artificially innervate muscles over time interval $t \in [0,T]$. If the i^{th} muscle acts about a single joint with angle $y_j(t)$, then the standard Hill type model gives the resulting moment as

$$\tau_{j,i}\big(u_i(t),y_j(t),\dot{y}_j(t)\big) = h_i(u_i(t),t)\,\tilde{F}_{M,j,i}\big(y_j(t),\dot{y}_j(t)\big) \tag{24}$$

where $h_i(u_i(t),t)$ is a Hammerstein structure comprising static non-linearity, $h_{IRC,i}(u_i(t))$, representing the isometric recruitment curve, cascaded with stable linear activation dynamics, $H_{LAD,i}$. Bounded term $\tilde{F}_{M,j,i}(\cdot)$ captures the effect of joint angle and angular velocity on the moment generated. As multiple muscles and/or tendons may each span any subset of joints, the general expression for the total moment produced about the j^{th} joint is represented by

$$\tau_j\big(u(t),y(t),\dot{y}(t)\big) = \sum_{i=1}^{m}\big\{d_{j,i}(y_j)\tau_{j,i}\big(u_i(t),y_j(t),\dot{y}_j(t)\big)\big\} \tag{25}$$

Here $d_{j,i}(y_j) = \frac{\partial E_i(y_j)}{\partial y_j}$ is the moment arm of the i^{th} muscle with respect to the j^{th} joint, where continuous function E is the associated excursion [25]. The overall moment $\tau \in \mathscr{L}^p_2[0,T]$ is therefore generated about the p joints of the inter-connected anthropomorphic and mechanical/robotic support structure, with associated joint angle signal $y \in \mathscr{L}^p_2[0,T]$. As shown in [7, chap. 2], this support structure can be represented by the rigid body system

$$B(y(t))\ddot{y}(t) + H(y(t),\dot{y}(t)) = \tau(u(t),y(t),\dot{y}(t)), \tag{26}$$

where $H(y(t),\dot{y}(t)) = C(y(t),\dot{y}(t))\dot{y}(t) + F(y(t),\dot{y}(t)) + G(y(t)) + R(y(t))$. Here $B(y(t))$ and $C(y(t),\dot{y}(t))$ are respectively the $p \times p$ inertial and Coriolis matrices of the amalgamated structure, and $G(y(t))$ is the $p \times 1$ combined gravity vector. The $p \times 1$ term $R(y(t))$ is the assistive moment produced by the mechanical passive/robotic support. Finally, $F(y(t),\dot{y}(t))$ is the $p \times 1$ anthropomorphic stiffness and damping vector representing joint stiffness, friction, and spasticity, which can be represented by the form

$$F(y(t),\dot{y}(t)) = F_e(y(t)) + F_v(\dot{y}(t)). \tag{27}$$

The next assumption is common in RT, and is satisfied by suitably adjusting the mechanical passive or robotic support.

Assumption 4.2 *Let system (26), (27) have forms $F_{e,i}(y(t)) = F_{e,i}(y_i(t))$, $F_{v,i}(\dot{y}(t)) = F_{v,i}(\dot{y}_i(t))$, $i = 1,\cdots,p$, and let support $R(y)$ be adjusted to satisfy the passivity condition*

$$(y-\bar{y})^\top\big(F_e(y) + G(y) + R(y) - \bar{\tau}\big) \geq 0 \tag{28}$$

for some signal pair $(\bar{\tau},\bar{y})$.

4.2 Operator Description of the Rehabilitation System

The stimulated arm system (24)-(27) equates to the map

$$N = H_{RB}F_m(y,\dot{y})H_{LAD}h_{IRC}, \tag{29}$$

with elements defined by the operators

$$\begin{aligned} h_{IRC} &: \mathscr{L}^m_2[0,T] \to \mathscr{L}^m_2[0,T] : u \mapsto y : y_i = h_{IRC,i}(u_i) \\ H_{LAD} &: \mathscr{L}^m_2[0,T] \to \mathscr{L}^m_2[0,T] : y \mapsto w : w_i = h_{LAD,i}y_i \\ F_m &: \mathscr{L}^m_2[0,T] \to \mathscr{L}^p_2[0,T] : w \mapsto \tau : \tau_i = \sum_j F_{M,i,j}w_j \end{aligned}$$

where $F_{M,i,j} = d_{i,j}(y_i)\,\tilde{F}_{M,i,j}(y_i(t),\dot{y}_i(t))$, $j = 1,\cdots,m$, and

$$H_{RB} : \mathscr{L}^p_2[0,T] \to \mathscr{L}^p_2[0,T] : \tau \mapsto y : \ddot{y} = B(y)^{-1}(\tau - H(y,\dot{y}))$$

4.3 Bounds on Muscle Fatigue

Since system (29) is BIBO stable (see Appendix A), we can directly specify Design Procedure 1 to yield a powerful design philosophy for rehabilitation. Within this, Theorem 3.1 and Theorem 3.2 bound specific sources of modeling error. The known structure of the system can be further exploited to yield more detailed, explicit bounds on common sources of uncertainty within the stimulated arm RT system. One of the most common sources is muscle fatigue, and is used next to illustrate the approach.

Proposition 4.3 *Suppose linear approximations to the dynamics H_{RB}, tendon function F_m and muscle curve h_{IRC}, given by $\overline{H_{RB}F}_m$ and $\bar{h}_{IRC}$ respectively, are used to construct nominal model $M = \overline{H_{RB}F}_m H_{LAD}\bar{h}_{IRC}$, which is subsequently used to design feedback controller K and ILC operator L satisfying (18) of Theorem 3.1. Then the system has a robust stability margin, and in particular is stable if*

$$\Delta_{IRC} < \sup_{k\in\mathbb{N}_+} \frac{b_{M//\bar{C}}^{-1} - \Delta_{RB}\|\bar{h}_{IRC}\|}{\|H_{RB}F_m|_{\bar{w}(k)}\|} \tag{30}$$

where the model mismatch due to muscle fatigue is

$$\Delta_{IRC} = \max_i \sup_{\|u\|\neq 0,\ k\in\mathbb{N}_+} \frac{\|(h_{IRC,i}|_{(\bar{u}(k))_i} - \bar{h}_{IRC,i})u\|}{\|u\|}$$

and the model mismatch due to linearization is

$$\Delta_{RB} = \sup_{\|u\|\neq 0,\ k\in\mathbb{N}_+} \frac{\|(H_{RB}F_m(y,\dot{y})|_{\bar{w}(k)} - \overline{H_{RB}F}_m)u\|}{\|u\|}.$$

Proof: See Appendix C. □

Proposition 4.3 bounds the allowable muscle fatigue which is characterised by the term Δ_{IRC}. This model mismatch increases as the patient experiences fatigue. The bound is given in terms of the modelling error due to linearization, which can be assumed to not vary. The feedback and/or ILC design can always be modified to ensure condition (30) is satisfied, e.g. by sacrificing convergence speed, and/or the range of frequencies over which convergence occurs. For the first time, Proposition 4.3 enables rehabilitation control systems to be designed to operate effectively in the presence of stipulated muscle fatigue bounds.

4.4 Experimental Results

Ten unimpaired participants were recruited and denoted P1 - P10 (aged 32 to 67 years). Each participant was instructed to provide no voluntary effort, and this was confirmed via surface electromyography measurement. Two pairs of 5 cm $\times$ 5 cm surface electrodes were positioned to stimulate nerves activating the anterior deltoid and triceps respectively. A 4×6 element fabric electrode array was positioned on the forearm with a cathode electrode positioned over the styloid process of the ulna. The system is shown in Figure 4. Two sets of electrode array elements were then chosen using a procedure described in [7] to correspond to wrist and finger extensors. The resulting four channels of ES ($m = 4$) comprised 40Hz square pulse trains whose pulsewidth was the controlled variable (0 - 300 μs). Each pulse train was generated by real-time hardware (dSPACE ds1103) and amplified by a modified commercial four channel voltage-controlled stimulator (Odstock Medical Ltd, UK). Two non-contact sensors

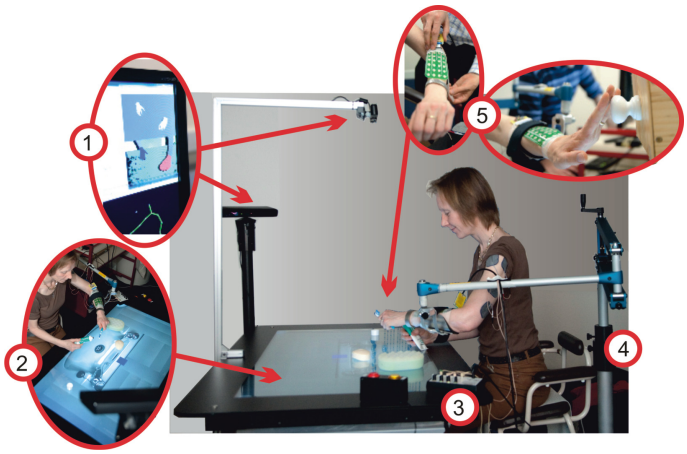

Fig. 4. System components: 1) Motion tracking hardware, 2) interactive touch table display, 3) ES controller and multiplexor hardware, 4) SaeboMAS and perching stool, and 5) electrode-array.

(Kinect and PrimeSense) were used to measure wrist, elbow and index finger flexion/extensor, together with shoulder elevation. Further details of the sensor accuracy, angle definitions and hardware appear in [7]. Two tasks were specified for each participant to perform: a light switch task and a drawer closing task. Each task was completed at two speeds: 5 seconds duration and 10 seconds duration. The approximate model M used for design was estimated at the beginning of the test session by applying ES sequences in an isometric identification test [13].

To achieve the two tasks, the model M was augmented to include joint velocity as well as position. Then the projection operator was defined using $q = 2$, $t_1 = t_2 = T$, with $P_1 = 0$, $P_2 = I$ to extract the position and velocity of the joints at the time instant $t = T$ only. Reference $\hat{y}^e$ then contained the position of the light switch or drawer. For each participant, feedback controller K was selected as a proportional-integral-derivative controller. Following this, the ILC form (5) with learning operator (22) was then implemented in the control scheme of Figure 1. Design Procedure 1 was applied to tune the parameters in order to balance tracking performance, convergence speed, and robustness to modeling uncertainty. Figure 5a) shows tracking results when the feedback controller K was chosen to have the small $b_{M//K}$ value of 2.35, and the ILC operator was chosen to have a larger gain bound of 3.72. Rapid ILC convergence can be

observed at the expense of more oscillatory learning transients. Figure 5b) shows the case where K was tuned with an increased $b_{M//K}$ value of 4.12, and the ILC convergence speed was reduced (via reduction of γ) to give a gain bound of 1.89. These results illustrate the use of Design Procedure 1 to manipulate the available robustness margin in practice.

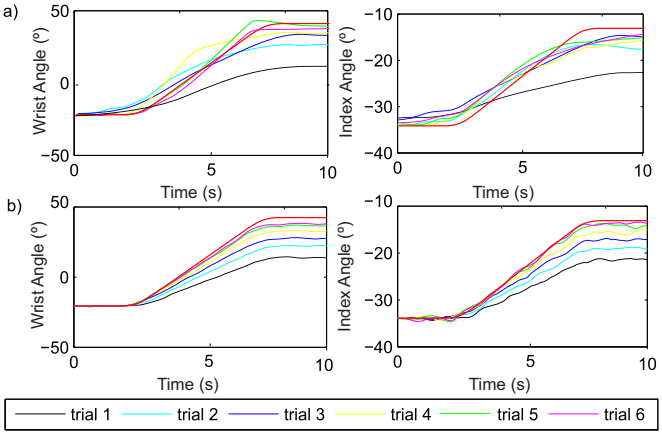

Fig. 5. Tracking results for light switch task using a) $b_{M//K} = 2.35$ and b) $b_{M//K} = 4.12$. Reference $\hat{y}^e$ is shown in red.

Results are shown in Table 1 for all participants, where the percentage error is computed using $100(\|e^e\|/\|\hat{y}^e\|)$. These confirm the efficacy of the general design procedure, and its suitability for rehabilitation in particular. All tasks were achieved accurately by allowing the designer to transparently manipulate robustness. Moreover they can also modify the task (through P) and effort that must be put into identifying an accurate model (through the stipulated gap bound) in meeting the condition of Theorem 3.1. The efficacy of the design procedure has led to its adoption in clinical practice [15].

	Percentage error			
	Light Switch		Drawer Close	
	Fast	Slow	Fast	Slow
P1	38.36, 7.03	35.29, 7.41	31.80, 12.78	41.83, 8.55
P2	34.75, 8.64	30.37, 10.12	35.01, 5.01	35.83, 12.46
P3	34.11, 7.21	36.69, 6.40	28.59, 8.24	29.76, 9.22
P4	32.62, 6.58	28.22, 9.76	39.31, 9.43	25.89, 5.68
P5	19.25, 4.85	35.37, 7.96	36.67, 9.38	28.09, 7.75
P6	27.26, 4.63	28.56, 9.44	43.18, 13.10	23.26, 9.34
P7	13.54, 4.47	32.54, 9.47	31.81, 7.44	30.64, 6.83
P8	23.20, 5.61	22.72, 3.82	26.45, 10.84	30.68, 11.76
P9	20.50, 5.19	17.85, 7.17	17.85, 7.20	17.85, 6.81
P10	16.87, 3.74	21.40, 6.50	20.74, 5.16	27.75, 14.03

Table 1
Percentage error during functional tasks ($k = 1$, $k = 6$).

5 Conclusions and Future Work

This paper establishes a principled framework for robust ILC design. By considering unstructured uncertainties, it considerably enlarges the scope of existing analysis in this field. Moreover, it embeds separate feedback control and ILC loops with each component utilizing the available robustness margins of the other to maximize overall performance. It thereby provides a mechanism for transparent control design which can balance performance and convergence speed. A substantial generalization is the inclusion of projection operator P which significantly enlarges the class of tasks that are supported. This provides the first robustness analysis to quantify the effect of the task on performance. To illustrate the framework's widespread applicability throughout ILC, it has been specified to the field of rehabilitation engineering where the difficulty in obtaining accurate models is particularly challenging. The use of projection P is also critical to support natural motor control motions required in clinical practice. Results have confirmed its efficacy and constitute the first robustness study in this domain.

The next stage of development is to extend the classes of feedback and ILC operators to nonlinear forms. The combined feedback and ILC framework will also be employed in practice within further clinical rehabilitation programmes with more functional movements (e.g. eating, brushing hair).

Acknowledgements

This work was supported by Engineering and Physical Sciences Research Council (EPSRC) Grant No. EP/M026388/1. Ethics Approval was given by University of Southampton Ethics and Research Governance Online (ERGO), ID 7710.

References

[1] H. S. Ahn, Y. Chen, and K. L. Moore. Iterative learning control: Brief survey and categorization. *IEEE Transactions on Systems, Man, and Cybernetics, Part C: Applications and Reviews*, 37(6):1099 –1121, nov. 2007.

[2] H. S. Ahn, K. L. Moore, and Y. Chen. Monotonic convergent iterative learning controller design based on interval model conversion. *IEEE Transactions on Automatic Control*, 51(2):366–371, 2006.

[3] P. M. Aubin, M. S. Cowley, and W. R. Ledoux. Gait simulation via a 6-DOF parallel robot with iterative learning control. *IEEE Transactions on Biomedical Engineering*, 55:1237–1240, 2008.

[4] J. Bae and M. Tomizuka. A gait rehabilitation strategy inspired by an iterative learning algorithm. *Mech*, 22(2):213–221, 2012.

[5] D. A. Bristow, M. Tharayil, and A. G. Alleyne. A survey of iterative learning control a learning-based method for high-performance tracking control. *IEEE Control Systems Magazine*, 26(3):96–114, 2006.

[6] T. Donkers, J. van de Wijdeven, and O. Bosgra. Robustness against model uncertainties of norm optimal iterative learning control. In *Proceedings of the 2008 American Control Conference*, pages 4561–4566, Seattle, WA, USA, 11-13 June 2008.

[7] C. T. Freeman. *Control System Design for Electrical Stimulation in Upper Limb Rehabilitation*. Springer International Publishing. Springer International Publishing, Switzerland, 2016.

[8] M. French. Robust stability of iterative learning control schemes. *International Journal of Robust and Nonlinear Control*, 18(10):1018–1033, 2008.

[9] T. T. Georgiou and M. C. Smith. Robustness analysis of nonlinear feedback systems: An input-output approach. *IEEE Transactions on Automatic Control*, 42(9):1200–1221, 1997.

[10] T. Harte, J. J. Hätönen, and D. H. Owens. Discrete-time inverse model-based iterative learning control: stability, monotonicity and robustness. *International Journal of Systems Science*, 78(8):557–586, 2005.

[11] P. Janssens, G. Pipeleers, and J. Swevers. A data-driven constrained norm-optimal iterative learning control framework for LTI systems. *IEEE Transactions on Control Systems Technology*, 21(2):546–551, 2013.

[12] M. Kutlu, C. T. Freeman, E. Hallewell, A.M. Hughes, and D.S Laila. Upper-limb stroke rehabilitation using electrode-array based functional electrical stimulation with sensing and control innovations. *Medical Engineering & Physics*, 38(4):366–379, 2016.

[13] F. Le, I. Markovsky, C. T. Freeman, and E. Rogers. Identification of electrically stimulated muscle models of stroke patients. *Control Engineering Practice*, 18(4):396–407, 2010.

[14] J. Lin and P. P. Varaiya. Bounded-input bounded-output stability of nonlinear time-varying discrete control systems. *IEEE Transactions on Automatic Control*, 12(4):423–427, 1967.

[15] K. L. Meadmore, T. Exell, E. Hallewell, A.-M. Hughes, C. T. Freeman, M. Kutlu, V. Benson, E. Rogers, and J. H. Burridge. The application of precisely controlled functional electrical stimulation to the shoulder, elbow and wrist for upper limb stroke rehabilitation: A feasibility study. *Journal of NeuroEngineering and Rehabilitation*, 11:105, 2014.

[16] J. H. Moon, T. Y. Doh, and M. J. Chung. A robust approach to iterative learning control design for uncertain systems. *Automatica*, 34(8):1001–1004, 1998.

[17] H. Nahrstaedt, T. Schauer, S. Hesse, and J. Raisch. Iterative learning control of a gait neuroprosthesis. *Automatisierungs*, 56(9):494–501, 2008.

[18] D. H. Owens, C. T. Freeman, and B. Chu. An inverse model approach to multivariable norm optimal iterative learning control with auxiliary optimization. *International Journal of Control*, 87(8):1646–1671, 2014.

[19] D. H. Owens, C. T. Freeman, and B. Chu. Generalized norm optimal iterative learning control with intermediate point and sub-interval tracking. *International Journal of Automation and Computing*, 12(3):243–253, 2015.

[20] D. De Roover and O. H. Bosgra. Synthesis of robust multivariable iterative learning controllers with application to a wafer stage motion system. *International Journal of Control*, 73(10):968–979, 2000.

[21] T. Seel, T. Schauer, and J. Raisch. Iterative learning control for variable pass length systems. In *IFAC World Congress*, pages 4880–4885, 2011.

[22] T. Seel, C. Werner, J. Raisch, and T. Schauer. Iterative learning control of a drop foot neuroprosthesis - generating physiological foot motion in paretic gait by automatic feedback control. *Control Engineering Practice*, 48:87–97, 2016.

[23] T. D. Son, H. S. Ahn, and K. L. Moore. Iterative learning control in optimal tracking problems with specified data points. *Automatica*, 49(5):1465–1472, 2013.

[24] A. Tayebi and M. B. Zeremba. Robust iterative learning control design is straight-forward for uncertain LTI systems satisfying teh robust performance condition. *IEEE Transactions on Automatic Control*, 48(1):101–106, 2003.

[25] F. J. Valero-Cuevas. A mathematical approach to the mechanical capabilities of limbs and fingers. *Progress in Motor Control*, 629:619–633, 2009.

[26] J. van de Wijdeven and O. Bosgra. Non-causal finite-time iterative learning control. In *Proceedings of the 46th IEEE Conference of Decision and Control*, 2007.

A Proof of Theorem 3.1

The required projection bound is given by

$$b_{\bar{M}//\bar{C}} = \|\Pi_{\bar{M}//\bar{C}}\|_{\binom{0}{\hat{y}}} = \sup_{\left\|\binom{u_0}{y_0}\right\|\neq 0} \frac{\left\|\Pi_{M//K}\binom{u_0}{y_0+\hat{y}} - \binom{\bar{u}}{\bar{y}}\right\|}{\left\|\binom{u_0}{y_0}\right\|}. \tag{A.1}$$

With the inclusion of disturbances u_0, y_0, the signals in Figure 2 (with N replaced by M) satisfy

$$\tilde{e}(i) = y_0(i) + \hat{y} - M\big(u_0(i) + K(v(i) + \tilde{e}(i))$$

It follows that

$$\begin{aligned}(I+MK)\big(\tilde{e}(i+1) - \tilde{e}(i)\big) &= \big(y_0(i+1) - y_0(i)\big) \\ &\quad - M\big(u_0(i+1) - u_0(i)\big) - MK\big(v(i+1) - v(i)\big)\end{aligned}$$

so that

$$\begin{aligned}\tilde{e}(i+1) = \big(I - (I+MK)^{-1}MKLP\big)\tilde{e}(i) + (I+MK)^{-1}\times \\ \big(y_0(i+1) - y_0(i)\big) - (I+MK)^{-1}M\big(u_0(i+1) - u_0(i)\big)\end{aligned}$$

which we can express recursively as

$$\begin{aligned}\tilde{e}(i+1) =& (I-GLP)^{i+1}\tilde{e}(0) + \sum_{j=0}^{i}(I-GLP)^j(I+MK)^{-1}\times \\ & (-M,I)\big(w_0(i+1-j) - w_0(i-j)\big)\end{aligned}$$

where $w_0(i) = (u_0(i), y_0(i))^\top$. It can be shown

$$\begin{aligned}\sum_{i=0}^{k}\tilde{e}(i) &= \tilde{e}(0) + \sum_{i=0}^{k-1}\tilde{e}(i+1) \\ &= \tilde{e}(0) + \sum_{i=0}^{k-1}(I-GLP)^{i+1}\tilde{e}(0) + \sum_{i=0}^{k-1}\sum_{j=0}^{i}(I-GLP)^j(I+MK)^{-1} \\ &\qquad \times (-M,I)\big(w_0(i+1-j) - w_0(i-j)\big) \\ &= \sum_{i=0}^{k}(I-GLP)^i\tilde{e}(0) + \sum_{i=0}^{k-1}\sum_{j=0}^{i}(I-GLP)^j(I+MK)^{-1}\times \\ &\qquad (-M,I)\big(w_0(i+1-j) - w_0(i-j)\big) \\ &= \sum_{i=0}^{k}(I-GLP)^i\tilde{e}(0) + \sum_{j=0}^{k-1}\Big\{(I-GLP)^j(I+MK)^{-1}(-M,I)\times \\ &\qquad \sum_{i=j}^{k-1}\big(w_0(i+1-j) - w_0(i-j)\big)\Big\} \\ &= \sum_{i=0}^{k}(I-GLP)^i\tilde{e}(0) + \sum_{j=0}^{k-1}\Big\{(I-GLP)^j(I+MK)^{-1}(-M,I) \\ &\qquad \big(w_0(k-j) - w_0(0)\big)\Big\}\end{aligned}$$

where we have used the identity

$$\sum_{i=0}^{k}\sum_{j=0}^{i}A^j y(i-j) = \sum_{j=0}^{k}A^j\sum_{i=0}^{k-j}y(i) = \sum_{j=0}^{k}A^j\sum_{i=j}^{k}y(i-j).$$

Hence, taking $v(0)=0, \tilde{e}(0)=(I+MK)^{-1}\big(\hat{y}+(-M,I)w_0(0)\big)$,

$$\begin{aligned}v(k+1)=&v(0)+LP\sum_{i=0}^{k}\tilde{e}(i)=LP\sum_{i=0}^{k}(I-GLP)^i(I+MK)^{-1}\hat{y}\\&+LP\sum_{i=0}^{k-1}(I-GLP)^i(I+MK)^{-1}(-M,I)w_0(k-i).\end{aligned}$$

Now

$$\begin{aligned}\tilde{e}(k+1)&=y_0(k+1)+\hat{y}-M\big(u_0(k+1)+K\big(v(k+1)\\&\qquad+\tilde{e}(k+1)\big)\big)\\&=(I+MK)^{-1}\hat{y}+(I+MK)^{-1}(-M,I)w_0(k+1)\\&=-(I+MK)^{-1}MKv(k+1)\end{aligned}\tag{A.2}$$

Therefore

$$\begin{aligned}v(k+1)+\tilde{e}(k+1)=&(I-G)v(k+1)+(I+MK)^{-1}\big(\hat{y}\\&+(-M,I)w_0(k+1)\big).\end{aligned}$$

We can then produce the plant input

$$\begin{aligned}u(k+1)=&u_0(k+1)+K\big(v(k+1)+\tilde{e}(k+1)\big)\\=&u_0(k+1)+K(I+MK)^{-1}\big(\hat{y}+(-M,I)w_0(k+1)\big)\\&+K(I-G)LP\Big(\sum_{i=0}^{k}(I-GLP)^i(I+MK)^{-1}\hat{y}+\\&\sum_{i=0}^{k-1}(I-GLP)^i(I+MK)^{-1}(-M,I)w_0(k-i)\Big)\\=&(I+KM)^{-1}(I,K)w_0(k+1)+K(I+MK)^{-1}\hat{y}+\\&K(I+MK)^{-1}LP\Big(\sum_{i=0}^{k}(I-GLP)^i(I+MK)^{-1}\hat{y}+\\&\sum_{i=0}^{k-1}(I-GLP)^i(I+MK)^{-1}(-M,I)w_0(k-i)\Big)\end{aligned}$$

We next employ the identity:

$$P\sum_{i=0}^{k}\big(I-GLP\big)^i=\sum_{i=0}^{k}\big(I-PGL\big)^iP\quad\forall\,k$$

to obtain

$$\begin{aligned}u(k+1)=&(I+KM)^{-1}(I,K)w_0(k+1)+K(I+MK)^{-1}\hat{y}+\\&K(I+MK)^{-1}L\Big(\sum_{i=0}^{k}(I-PGL)^iP(I+MK)^{-1}\hat{y}+\\&\sum_{i=0}^{k-1}(I-PGL)^iP(I+MK)^{-1}(-M,I)w_0(k-i)\Big)\end{aligned}\tag{A.3}$$

which, if condition (6) holds, ultimately produces the bound

$$\|\Pi_{\bar{M}//\bar{C}}\|_{\binom{0}{\hat{y}}}\leq\frac{\left\|\binom{I}{M}K(I+MK)^{-1}L\right\|\|P(I+MK)^{-1}(-M,I)\|}{1-\|I-PGL\|}+b_{M//K}\tag{A.4}$$

Next use the identity:

$$L\sum_{i=0}^{k}\big(I-PGL\big)^i=\sum_{i=0}^{k}\big(I-LPG\big)^iL\quad\forall\,k\tag{A.5}$$

and substitute it into (A.3) to obtain

$$\begin{aligned}u(k+1)=&(I+KM)^{-1}(I,K)w_0(k+1)+K(I+MK)^{-1}\hat{y}+\\&K(I+MK)^{-1}\Big(\sum_{i=0}^{k}(I-LPG)^iLP(I+MK)^{-1}\hat{y}+\\&\sum_{i=0}^{k-1}(I-LPG)^iLP(I+MK)^{-1}(-M,I)w_0(k-i)\Big)\end{aligned}$$

which, if condition (8) holds, ultimately produces the bound

$$\|\Pi_{\bar{M}//\bar{C}}\|_{\binom{0}{\hat{y}}}\leq\frac{\left\|\binom{I}{M}K(I+MK)^{-1}\right\|\|LP(I+MK)^{-1}(-M,I)\|}{1-\|I-LPG\|}+b_{M//K}\tag{A.6}$$

Hence (18) is an upper bound for both (A.4) and (A.6). The final result follows by applying the gap bounds of [9].

B Proof of Theorem 3.2

First denote the sequence of operating point trajectories generated by $[\bar{M},\bar{C}]$ in the absence of disturbance as $\binom{\bar{u}_1}{\bar{y}_1}=\Pi_{\bar{M}//\bar{C}}\binom{0}{\hat{y}}$, and likewise $\binom{\bar{u}}{\bar{y}}=\Pi_{\bar{N}//\bar{C}}\binom{0}{\hat{y}}$ is the sequence of operating point trajectories generated by $[\bar{N},\bar{C}]$ in the absence of disturbance. Define the lifted graphs

$$\begin{aligned}\mathscr{G}_{\bar{M}}:=\Big\{\binom{u}{y}:\left\|\binom{u}{y}\right\|_{\binom{\bar{u}_1}{\bar{y}_1}}=\Big(\sum_{k=0}^{\infty}\left\|\binom{u(k)}{y(k)}\right\|^2_{\binom{\bar{u}_1(k)}{\bar{y}_1(k)}}\Big)^{\frac{1}{2}}<\infty,\\y(k)=Mu(k)\Big\},\\\mathscr{G}_{\bar{N}}:=\Big\{\binom{u}{y}:\left\|\binom{u}{y}\right\|_{\binom{\bar{u}}{\bar{y}}}=\Big(\sum_{k=0}^{\infty}\left\|\binom{u(k)}{y(k)}\right\|^2_{\binom{\bar{u}(k)}{\bar{y}(k)}}\Big)^{\frac{1}{2}}<\infty,\\y(k)=Nu(k)\Big\}.\end{aligned}$$

A map $\bar{\Psi}:\mathscr{G}_{\bar{M}}\mapsto\mathscr{G}_{\bar{N}}$ is surjective if $\forall\, y\in\mathscr{G}_{\bar{N}}\ \exists\, x\in\mathscr{G}_{\bar{M}}$ such that $\bar{\Psi}(x)=y$. Let us choose an element $y\in\mathscr{G}_{\bar{N}}$ where $y(k)=\begin{pmatrix}u(k)+\bar{u}(k)\\N(u(k)+\bar{u}(k))\end{pmatrix}$ for some $\|u\|<\infty$. It follows that $\|u+\bar{u}\|_{\bar{u}}<\infty$, and since N is bounded $\|N(u+\bar{u})\|_{\bar{u}}=\|y+\bar{y}\|_{\bar{y}}<\infty$. We therefore define the map $y(k)=(\bar{\Psi}x)(k)=\Psi_k(x(k))=\Psi_k\Big(\begin{smallmatrix}u(k)+\bar{u}_1(k)\\M(u(k)+\bar{u}_1(k))\end{smallmatrix}\Big)=\Big(\begin{smallmatrix}u(k)+\bar{u}(k)\\N(u(k)+\bar{u}(k))\end{smallmatrix}\Big)$. Since M is bounded $\|x(k)\|_{\binom{\bar{u}(k)}{\bar{y}(k)}}=\left\|\Big(\begin{smallmatrix}u(k)+\bar{u}_1(k)\\M(u(k)+\bar{u}_1(k))\end{smallmatrix}\Big)\right\|_{\binom{\bar{u}_1(k)}{\bar{y}_1(k)}}=\left\|\binom{u(k)}{y(k)}\right\|<\infty\ \forall\ k.$

Hence $x\in\mathscr{G}_{\bar{M}}$ and we note $\bar{\Psi}\binom{\bar{u}_1}{\bar{y}_1}=\binom{\bar{u}}{\bar{y}}$. The non-linear biased gap metric measures the mismatch between plant model M and true system N, and is defined as

$$\begin{aligned}\delta(\bar{M},\bar{N}):=\inf\Big\{\|(\bar{\Psi}-I)_{\mathscr{G}_{\bar{M}}}\|_{\binom{\bar{u}_1}{\bar{y}_1}}:\bar{\Psi}\text{ is a causal, surjective}\\\text{map from }\mathscr{G}_{\bar{M}}\text{ to }\mathscr{G}_{\bar{N}}\text{ with }\bar{\Psi}\binom{\bar{u}_1}{\bar{y}_1}=\binom{\bar{u}}{\bar{y}}\Big\},\end{aligned}\tag{B.1}$$

It therefore follows that

$$\delta(\bar{M},\bar{N}) \leq \sup_{x\in\mathscr{G}_{\bar{M}}\setminus\{0\}} \frac{\Big(\sum_{k=0}^{\infty}\Big\|(\Psi_k-I)x(k)-(\Psi_k-I)\begin{pmatrix}\bar{u}_1(k)\\ \bar{y}_1(k)\end{pmatrix}\Big\|^2\Big)^{\frac{1}{2}}}{\Big(\sum_{k=0}^{\infty}\Big\|x(k)-\begin{pmatrix}\bar{u}_1(k)\\ \bar{y}_1(k)\end{pmatrix}\Big\|^2\Big)^{\frac{1}{2}}}$$

$$\leq \sup_{\|u\|\neq 0} \frac{\begin{array}{r}(\sum_{k=0}^{\infty}\|(N(u(k)+\bar{u}(k))-N\bar{u}(k))-\\ (M(u(k)+\bar{u}_1(k))-M\bar{u}_1(k))\|^2)^{\frac{1}{2}}\end{array}}{\|u\|}$$

$$= \sup_{\|u\|\neq 0} \frac{(\sum_{k=0}^{\infty}\|\big(N|_{\bar{u}(k)}-M\big)u(k)\|^2)^{\frac{1}{2}}}{\|u\|}$$

$$\leq \sup_{\|u\|\neq 0} \frac{\Big(\sum_{k=0}^{\infty}\Big(\sup_{\|u(k)\|\neq 0}\frac{\big\|\big(N|_{\bar{u}(k)}-M\big)u(k)\big\|^2}{\|u(k)\|^2}\Big)\|u(k)\|^2\Big)^{\frac{1}{2}}}{\|u\|}$$

$$\leq \sup_{\|u\|\neq 0} \frac{\Big(\sup\limits_{\substack{\|v\|\neq 0\\ k\in\mathbb{N}_+}}\frac{\big\|\big(N|_{\bar{u}(k)}-M\big)v\big\|}{\|v\|}\Big)\Big(\sum_{k=0}^{\infty}\|u(k)\|^2\Big)^{\frac{1}{2}}}{\|u\|}$$

$$= \sup_{k\in\mathbb{N}_+}\Big(\sup_{\|v\|\neq 0}\frac{\big\|\big(N|_{\bar{u}(k)}-M\big)v\big\|}{\|v\|}\Big)$$

C Proof of Proposition 4.3

The first ancillary result establishes that all joints are passive about operating point $(\bar{\tau},\bar{y})$ if Assumption 4.2 holds.

Proposition C.1 *Let function $F(y,\dot{y})$ have form (27) and let the robotic or passive support structure be designed to satisfy Assumption 4.2. Then the rigid body system*

$$B(y)\ddot{y}+C(y,\dot{y})\dot{y}+F(y,\dot{y})+G(y)+R(y)=\tau, \qquad \text{(C.1)}$$

with input τ and output y, is BIBO stable about $(\bar{\tau},\bar{y})$.

Proof: Following [14] we impose additional conditions on a suitable Liapunov function to enable asymptotic stability to be exchanged for the stricter condition of BIBO stability. Taking for simplicity $\dot{\bar{y}}=0$, operating point $\bar{y}$ satisfies

$$R(\bar{y})+G(\bar{y})+F_e(\bar{y})=\bar{\tau}, \qquad \text{(C.2)}$$

and the system dynamics can be represented by

$$\begin{array}{l}B(\tilde{y}+\bar{y})\ddot{y}+C(\tilde{y}+\bar{y},\dot{y})\dot{y}+R(\tilde{y}+\bar{y})+G(\tilde{y}+\bar{y})+\\ F_v\dot{y}+F_e(\tilde{y}+\bar{y})-R(\bar{y})-G(\bar{y})-F_e(\bar{y})=\tau-\bar{\tau}\end{array} \qquad \text{(C.3)}$$

where $\tilde{y}=y-\bar{y}$, with $\dot{\tilde{y}}=\dot{y}$, $\ddot{\tilde{y}}=\ddot{y}$. Since (28) holds we select the symmetric positive-definite Liapunov function

$$V(\tilde{y},\dot{y})=\dot{y}^\top\frac{B(\tilde{y}+\bar{y})}{2}\dot{y}+\int_0^{\tilde{y}}\big(F_e(\sigma)+G(\sigma)+R(\sigma)-F_e(\bar{y})-R(\bar{y})-G(\bar{y})\big)\delta\sigma$$

so that

$$\begin{aligned}\dot{V}(\tilde{y}(t),\dot{y}(t)) =&\dot{y}(t)^\top B(\tilde{y}(t)+\bar{y}(t))\ddot{y}(t)+\\ &\dot{y}(t)^\top\frac{\dot{B}(\tilde{y}(t)+\bar{y}(t))}{2}\dot{y}(t)+\dot{y}(t)^\top\big(F_e(\tilde{y}(t)+\bar{y}(t))\\ &+G(\tilde{y}(t)+\bar{y}(t))+R(\tilde{y}(t)+\bar{y}(t)\big)-\\ &\dot{y}(t)^\top\big(F_e(\bar{y}(t))+G(\bar{y}(t))+R(\bar{y}(t))\big)\\ =&\dot{y}(t)^\top\Big(\frac{\dot{B}(y(t))}{2}-C(y(t),\dot{y}(t))-F_v\Big)\dot{y}(t)+\\ &\dot{y}(t)^\top(\tau(t)-\bar{\tau}(t)).\end{aligned}$$

Since $\frac{1}{2}\dot{B}(y(t))-C(y(t),\dot{y}(t))$ is skew-symmetric, $\frac{\dot{B}(y(t))}{2}-C(y(t),\dot{y}(t))-F_v$ is negative definite since F_v has positive diagonal entries. Hence $\exists\,\alpha>0$ such that

$$\dot{y}(t)^\top\Big(\frac{\dot{B}(y(t))}{2}-C(y(t),\dot{y}(t))-F_v\Big)\dot{y}(t)\leq-\alpha\big\|\dot{y}(t)\big\|^2$$

which gives the bound

$$\begin{aligned}\dot{V}(\tilde{y}(t),\dot{y}(t)) &\leq -\alpha\big\|\dot{y}(t)\big\|^2+\big\|\dot{y}(t)\big\|\big\|\tau(t)\big\|_{\bar{\tau}}\\ &\leq -\big\|\dot{y}(t)\big\|\Big(\alpha\big\|\dot{y}(t)\big\|-\big\|\tau(t)\big\|_{\bar{\tau}}\Big).\end{aligned} \qquad \text{(C.4)}$$

Now note that for all bounded $\tau(t)$

$$\big\|\dot{y}(t)\big\|\geq\frac{\|\tau(t)\|_{\bar{\tau}}}{\alpha}\Rightarrow\dot{V}(\tilde{y}(t),\dot{y}(t))\leq 0 \qquad \text{(C.5)}$$

and since $B(\cdot)$ and $C(\cdot)$ are bounded and continuous, $\big\|\tilde{y}(t)\big\|$ is bounded when $\big\|\dot{y}(t)\big\|<\frac{\|\tau(t)\|_{\bar{\tau}}}{\alpha}$, with $\|\tau\|_{\bar{\tau}}=0\Rightarrow y=\bar{y}$ so that $\big\|y-\bar{y}\big\|\leq\gamma_1\|\tau\|_{\bar{\tau}}$ for some finite γ_1. Then, through application of LaSalle's Invariance Principle, for each τ there exists a finite γ_2 such that

$$\big\|\dot{y}\big\|\geq\frac{\|\tau\|_{\bar{\tau}}}{\alpha}\Rightarrow\|\tilde{y}\|\leq\gamma_2\|\tau\|_{\bar{\tau}}. \qquad \text{(C.6)}$$

Combining the above cases guarantees $\forall\tau$

$$\|y\|_{\bar{y}}\leq\max\{\gamma_1,\gamma_2\}\|\tau\|_{\bar{\tau}} \qquad \text{(C.7)}$$

and it follows that system (C.1) is BIBO stable about $(\bar{\tau},\bar{y})$.

Hence Theorem 3.1 may be applied using the forms $N|_{\bar{u}(k)}=H_{RB}F_m(y,\dot{y})|_{\bar{w}}H_{LAD}h_{IRC}|_{u(k)}$ and $M=\overline{H_{RB}F}_mH_{LAD}\bar{h}_{IRC}$ within definition (21). From (17) this gives the requirement

$$\sup_{\substack{\|u\|\neq 0\\ k\in\mathbb{N}_+}}\frac{\begin{array}{r}\|(H_{RB}F_m(y,\dot{y})|_{\bar{w}(k)}H_{LAD}h_{IRC}|_{u(k)}\\ -\overline{H_{RB}F}_mH_{LAD}\bar{h}_{IRC})u\|\end{array}}{\|u\|}<b_{\bar{M}//\bar{C}}^{-1}.$$

Taking, without loss of generality $\|H_{LAD}\|=1$, the left hand side is bounded by

$$\sup_{\|u\|\neq 0}\frac{\|\bar{h}_{IRC}u\|}{\|u\|}\sup_{\substack{\|u\|\neq 0\\ k\in\mathbb{N}_+}}\frac{\|(H_{RB}F_m(y,\dot{y})|_{\bar{w}(k)}-\overline{H_{RB}F}_m)u\|}{\|u\|}+$$

$$\sup_{\substack{\|u\|\neq 0\\ k\in\mathbb{N}_+}}\frac{\|(h_{IRC}|_{u(k)}-\bar{h}_{IRC})u\|}{\|u\|}\sup_{\substack{\|u\|\neq 0\\ k\in\mathbb{N}_+}}\frac{\|H_{RB}F_m(y,\dot{y})|_{\bar{w}(k)}u\|}{\|u\|}$$